RESEARCH ARTICLE | FEBRUARY 01 2023

Structural, magnetic, and magnetocaloric characterization of NiMnSn microwires prepared by Taylor-Ulitovsky technique

Special Collection: 67th Annual Conference on Magnetism and Magnetic Materials

M. L. Arreguín-Hernández ; M. Varga; M. Hennel ; A. Dzubinska ; T. Ryba; M. Reiffers ; P. Diko; J. L. Sánchez Llamazares ; R. Varga

AIP Advances 13, 025101 (2023)
https://doi.org/10.1063/9.0000549

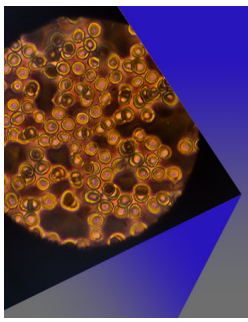

Structural, magnetic, and magnetocaloric characterization of NiMnSn microwires prepared by Taylor-Ulitovsky technique

Cite as: AIP Advances 13, 025101 (2023); doi: 10.1063/9.0000549
Submitted: 3 October 2022 • Accepted: 10 November 2022 •
Published Online: 1 February 2023

M. L. Arreguín-Hernández,[1,2,a] M. Varga,[1,3] M. Hennel,[1,3] A. Dzubinska,[1] T. Ryba,[4] M. Reiffers,[5] P. Diko,[6] J. L. Sánchez Llamazares,[2,7,a] and R. Varga[1,4]

AFFILIATIONS

[1] CPM-TIP, UPJS, 041 01 Kosice, Slovakia
[2] Instituto Potosino de Investigación Científica y Tecnológica A.C., Camino a la Presa de San José 2055, Col. Lomas 4a, San Luis Potosí S.L.P. 78216, Mexico
[3] Institute of Physics, Faculty of Science, UPJS, Park Angelinum 9, 040 01 Kosice, Slovakia
[4] RVmagnetic, Hodkovce 21, 044 21 Hodkovce, Slovakia
[5] Faculty of Humanities and Natural Sciences, University of Presov, Ul. 17. Novembral, 080 01 Presov, Slovakia
[6] Institute of Esperimental Physics, Watsonova 47, 040 01 Kosice, Slovakia
[7] Departamento de Fisica, Universidad de Oviedo, 33007 Oviedo, Spain

Note: This paper was presented at the 67th Annual Conference on Magnetism and Magnetic Materials.
[a] **Authors to whom correspondence should be addressed:** maria.arreguin@ipicyt.edu.mx and jose.sanchez@ipicyt.edu.mx

ABSTRACT

We report the structural, magnetic, and magnetocaloric characterization of glass-coated $Ni_{42.9}Mn_{37.1}Sn_{20.0}$ microwires produced by the Taylor-Ulitovsky method. Microwire samples crystallized into a single-phase austenite with the $L2_1$-type crystal structure (space group $Fm\bar{3}m$, lattice parameter $a \approx 6.02$ Å) and a Curie temperature of 349 K. A distinctive feature of the produced microwires is that saturation magnetization is reached at a very low magnetic field (~0.15 T). For a magnetic field change of 3 T, the produced microwires showed a reversible maximum magnetic entropy change $|\Delta S_M|^{max}$ of 2.3 J kg^{-1} K^{-1} and a refrigerant capacity of 197 J kg^{-1}, which are similar to the values reported by other austenitic NiMnSn alloys produced by rapid quenching techniques.

Heusler-type Ni–Mn–X (X = Ga, In, Sn, and Sb) alloys have been the focus of considerable attention in the last 20 years due to their multifunctional properties linked to the first-order martensitic-like phase transition that each of these systems shows for a given restricted compositional interval.[1] The observation of giant magnetocaloric and mechano-caloric effects in alloys derived from these ternary alloy systems has been one of the most important research branches encouraged by the interest in developing new solid-state refrigeration devices. Depending on the chemical composition, the martensitic transformation may lead to a magnetostructural transformation from a ferromagnetic austenite to a ferromagnetic or weak magnetic martensite.[1,2] Otherwise, the alloy crystallizes into a ferromagnetic austenite for which the Curie temperature (T_C^A) lies around room temperature.[1,2] In this system, austenite may present either a cubic highly ordered $L2_1$-type or disordered B2-type crystal structure.[2,3]

From the viewpoint of caloric effect applications, microwire shape brings the significant advantage of a high surface-to-volume ratio; in addition, some works report on a significant reduction of the magnetic field needed to reach saturation magnetization suggesting that a substantial shape anisotropy is induced along the microwire cylindrical axis during the fabrication process.[4–9] However, to date, little information exists about the synthesis and properties of (Ni–Mn)-based Heusler-type magnetic microwires. Moreover, previous investigations on the magnetic and magnetocaloric properties of (Ni–Mn)-based microwires have mainly

focused on alloys undergoing a magnetostructural martensitic transformation and the properties related to it.[4–10] The Taylor-Ulitovsky technique can produce long and continuous glass-coated microwires.[11] The coating not only helps to avoid undesirable effects such as oxidation but also to improve the microwires' mechanical stability which is one of the main drawbacks of these materials for applications due to their fragility. The manipulation is also facilitated by the glass coating.

In the present work, we report the synthesis of single-phase austenitic Ni–Mn–Sn microwires together with the characterization of their structural, magnetic, and magnetocaloric properties (the latter were assessed through the second-order ferromagnetic transition of austenite). They were produced by the Taylor-Ulitovsky technique and studied by X-ray diffraction, scanning electron microscopy (SEM), and magnetization measurements.

First, a bulk arc-melted alloy with a nominal composition of $Ni_{50}Mn_{25}Sn_{25}$ was prepared from pure elements (99.9% or better) under a highly pure argon atmosphere. A 10% wt. of Mn was added to compensate for the loss by evaporation in both the arc melting and Taylor-Ulitovsky processes. The sample was flipped and melted several times to improve its starting chemical homogeneity. From this ingot, a long glass-coated microwire was fabricated by the Taylor-Ulitovsky method. The microstructure and elemental chemical composition were studied in a VEGA 3 TESCAN scanning electron microscope (SEM) equipped with an energy-dispersive spectroscopy (EDS) system. The X-ray diffraction (XRD) pattern at room temperature was recorded in a Rigaku D/MAX Rapid II diffractometer with MoK_α radiation. Before to XRD analysis, the glass was removed from the microwire. Magnetization measurements were performed by vibrating sample magnetometry (VSM) in a Quantum Design PPMS VersaLab system. These measurements were done for a 7 mm long glass-free single microwire; the magnetic field was applied parallel to the longitudinal or fabrication direction to make the internal demagnetizing magnetic field negligible.

The SEM micrographs of Fig. 1(a) show a typical view of the physical dimensions and polycrystalline nature of the fabricated microwires (which are formed by micronic in size grains). The average diameter of the metallic nucleus was around 140–160 μm; the average was determined by SEM observation of the cross-section of six different microwire sample pieces. Semiquantitative EDS analyses performed on several microwire pieces revealed a shift of the elemental chemical composition from the nominal value (50:25:25) to Ni 42.9 at. %, Mn 37.1 at. %, and Sn: 20.0 at. % (with an approximate error in the determination of 0.2 at. %).

Fig. 2(a) shows the XRD pattern recorded for a single glass-free microwire. All the diffraction peaks were correctly indexed based on a cubic $L2_1$-type crystal structure with space group $Fm\bar{3}m$. Notice that high-intensity reflections appear for Miller indices (111), (200), (220), (422), (440), and (620) (located at 2θ values of 11.9°,

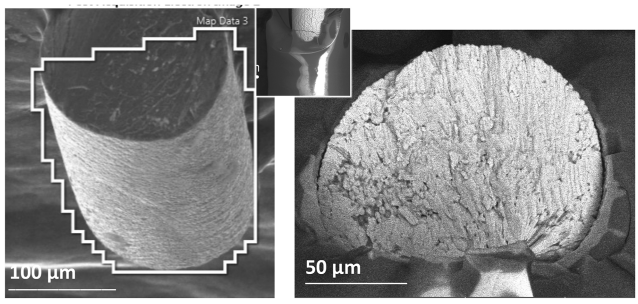

FIG. 1. SEM images showing the cross-section of the produced microwires.

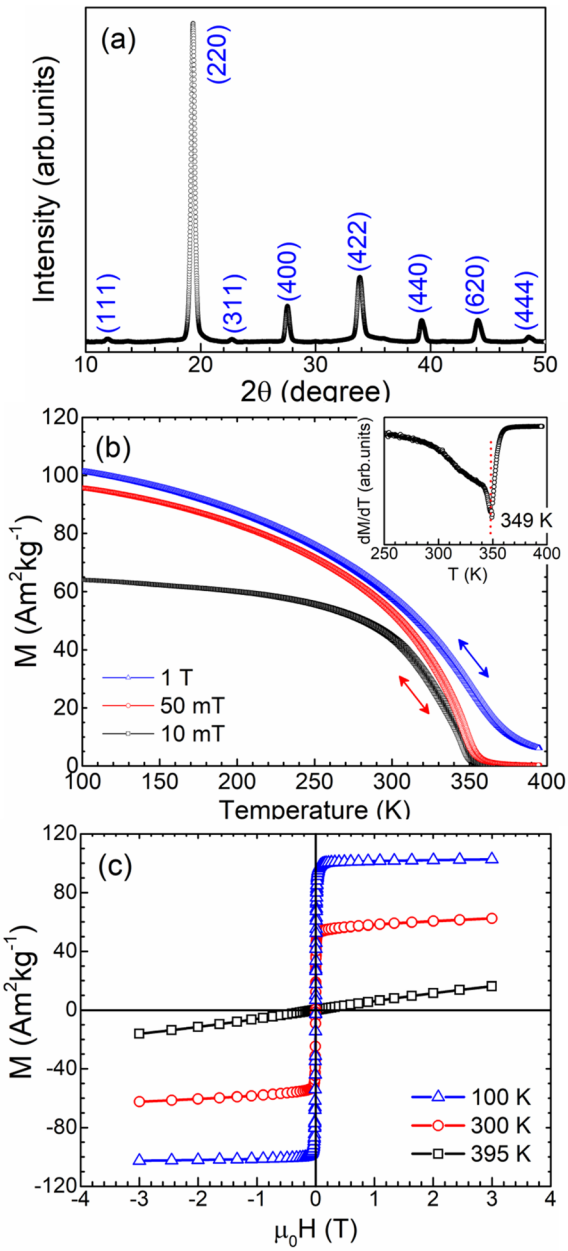

FIG. 2. Room temperature X-ray diffraction pattern (a), $M(T)$ curves measured on cooling and heating at different magnetic fields as the double arrows indicate (Inset: $dM/dT(T)$ curve at 10 mT) (b), and hysteresis loops measured at different temperatures (c) for the produced microwires.

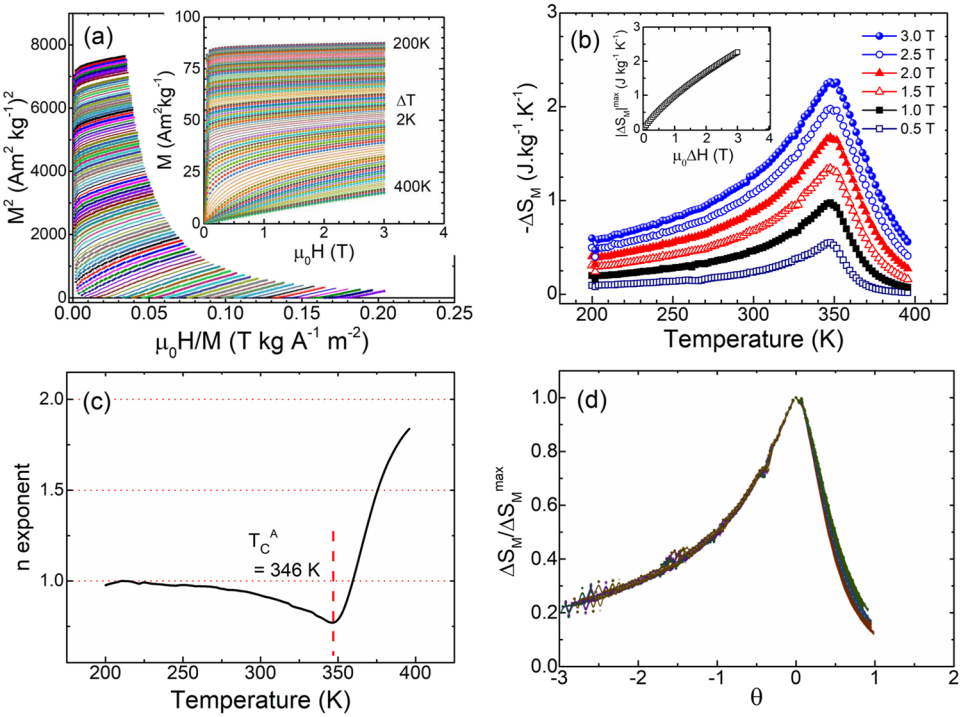

FIG. 3. Arrott plots (a) and the set of isothermal magnetization curves from which they were obtained (inset), $\Delta S_M(T)$ curves for applied magnetic field changes ranging from 0.5 to 3.0 T (b), temperature dependence of exponent n (c), and universal $\Delta S_M/\Delta S_M{}^{max}$ curves (d) obtained for the produced microwires.

13.7°, 19.4°, 33.8°, 39.3°, and 44.2°, respectively). The lattice parameter a calculated for the $L2_1$-type structure was 6.02 Å, which is close to the one reported in Ref. 2 for the $Ni_{50}Mn_{30}Sn_{20}$ bulk alloy (6.024 Å). Fig. 2(b) displays the thermomagnetic $M(T)$ curves measured on heating and cooling from 100 to 395 K under static magnetic fields of 10 mT, 50 mT, and 1 T (the temperature sweep rate was 1.0 K min^{-1}). From the minimum in the $dM/dT(T)$ curve measured at 10 mT, plotted at the inset of the figure, we found a Curie temperature $T_C{}^A$ for austenite of 349 K. This value is slightly above the 340 K value reported in Ref. 2 for the $Ni_{50}Mn_{30}Sn_{20}$ bulk alloy but is in good correspondence with the $T_C{}^A$ dependence with the average valence electron concentration per atom e/a reported in Ref. 1 (for $Ni_{50}Mn_{30}Sn_{20}$ e/a equals 7.906 vs 7.7 for the microwires). It is also worth noting the little difference in magnetization between the $M(T)$ curves measured at 50 mT and 1.0 T. This denotes that saturation magnetization is reached at a low magnetic field strength (around 0.15 T), as better viewed in the magnetic rectangular-shaped hysteresis loops measured at 100 and 300 K of Fig. 2(c). This feature suggests that the easy magnetization direction of the grains in the microwire tends to be parallel to the wire cylindrical axis, a fact that could be a result of the could be a result of the tensile stress applied to the alloy during solidification and glass-coating processes.

The inset of Fig. 3(a) shows the set of isothermal magnetization $M(\mu_0 H)$ curves measured from 200 to 400 K (one each 2 K) up to a maximum magnetic field of 3 T across the magnetic transition. The second-order nature of the magnetic transition is highlighted by the foreground graph that shows the Arrott plots progressively changing their concavity, from negative to positive, when the temperature increases from the ferro to the paramagnetic region (below and above 349 K, respectively). From the set of isotherms, the thermal dependencies of the magnetic entropy change, the $\Delta S_M(T)$ curves, were obtained numerically integrating the Maxwell relation. They are shown in Fig. 3(b), together with the magnetic field change dependence of $|\Delta S_M|^{max}$ (shown in the inset). As previously stated, their remarkable feature is their saturation at low magnetic fields in the ferromagnetic region. The refrigerant capacity RC was determined as follows: (a) RC-1 from the product $|\Delta S_M|^{max} \times \delta T_{FWHM}$, where δT_{FWHM} is the full-width at half-maximum of the $\Delta S_M(T)$ curve (i.e. $\delta T_{FWHM} = T_{hot} - T_{cold}$), and; (b) RC-2 calculating the area below the $\Delta S_M(T)$ curve between T_{hot} and T_{cold} (i.e., $RC - 2 = \int_{T_{cold}}^{T_{hot}} \Delta S_M(T) dT$).[12] The most significant values of the magnetocaloric properties of the produced microwires are summarized in Table I; for the sake of comparison, the table also lists the reported $|\Delta S_M|^{max}$ and RC values for austenite in alloys produced by rapid solidification. $|\Delta S_M|^{max}$ and RC reached similar values to those reported in the literature for Ni–Mn–Sn alloy produced by rapid quenching methods.[4,13,14]

For materials with second-order phase transition, $|\Delta S_M|^{max}$ follows the scaling law $|\Delta S_M|^{max} \propto (\mu_0 \Delta H)^n$, where n is a critical exponent (that for ferromagnets following the mean-field model equals 0.66), and the relationship $\Delta S_M/\Delta S_M(T_r)$ vs the rescaled temperature θ, defined as $\theta = (T - T_C)/(T_r - T_C)$, should collapse into the universal curve.[15] Fig. 3(c) displays the temperature dependence of n whereas Fig. 3(d) shows the experimentally determined universal curve. For the present samples n = 0.76

TABLE I. Comparison of $|\Delta S_M|^{max}$, *RC*-1, and *RC*-2 and values obtained for $Ni_{42.9}Mn_{37.1}Sn_{20.0}$ microwires with data reported in the literature for austenite in other (Ni–Mn)-based alloys produced by rapid solidification techniques.

Alloy composition	$T_C{}^A$ (K)	$\mu_0\Delta H$ (T)	$\lvert\Delta S_M\rvert^{max}$ (J kg^{-1} K^{-1})	*RC*-1 (J kg^{-1})	*RC*-2 (J kg^{-1})	References
$Ni_{42.9}Mn_{37.1}Sn_{20.0}$	349	3	2.3	197	145	This work
Microwires		2	1.7	123	92	
$Ni_{50}Mn_{37}Sn_{13}$ ribbons	315	1.8	1.4–1.9	···	45-56	13
$Ni_{45.6}Fe_{3.6}Mn_{38.4}Sn_{12.4}$ microwires	298	2	2.0	175	215	14
$Ni_{49}Mn_{23.5}In_{17.5}$ microwires	246	3	2.0	···	120	4

(at 346 K), which is slightly above the expected value for an ideal ferromagnet.

To conclude, this work demonstrates the feasibility of the Taylor-Ulitovsky technique to fabricate single-phase glass-coated austenitic microwires in the Ni–Mn–Sn system that can be mechanically manipulated due to the ductility provided by the glass sheath. Austenite crystallized into a highly ordered $L2_1$-type crystal structure with a Curie temperature slightly above room temperature showing magnetocaloric properties linked to the second-order magnetic transition, which compare favorably with those reported for this phase in alloys with a similar composition. The isothermal magnetization curves suggest the preferential orientation of the easy magnetization direction of the micronic grains in the microwires along the fabrication direction, opening a way to further optimization via the adequate control of the processing parameters.

ACKNOWLEDGMENTS

Work supported by Slovak Grant Agency VEGA 1/0053/19 (APVV-16-0079), SEP-CONACyT, Mexico (research grant A1-S-37066), and Laboratorio Nacional de Nanociencias y Nanotecnologia (LINAN, IPICyT). M. L. Arreguín-Hernández is grateful to The National Scholarship Programme of the Slovakia Republik for the scholarship granted, and to CONACyT for supporting her Ph.D. studies (fellowship No. 861512). J. L. Sánchez Llamazares acknowledges the support received from the European Union-NextGenerationEU, Ministerio de Universidades, and Plan de Recuperación, Transformación y Resiliencia, in the framework of the Maria Zambrano program of the University of Oviedo, Asturias, Spain (Reference: MU-21-UP2021-030 71741542).

AUTHOR DECLARATIONS

Conflict of Interest

The authors have no conflicts to disclose.

Author Contributions

M. L. Arreguín-Hernández: Conceptualization (equal); Data curation (equal); Formal analysis (equal); Funding acquisition (equal); Investigation (equal); Methodology (equal); Writing – original draft (equal). **M. Varga**: Data curation (equal); Formal analysis (equal); Funding acquisition (equal); Investigation (equal); Methodology (equal); Software (equal); Validation (equal); Writing – original draft (equal). **M. Hennel**: Data curation (equal); Formal analysis (equal); Funding acquisition (equal); Methodology (equal); Software (equal); Validation (equal); Writing – original draft (equal). **A. Dzubinska**: Funding acquisition (equal); Methodology (equal); Software (equal). **T. Ryba**: Methodology (equal); Resources (equal). **M. Reiffers**: Resources (equal). **P. Diko**: Resources (equal). **J. L. Sánchez Llamazares**: Investigation (equal); Project administration (equal); Resources (equal); Supervision (equal); Validation (equal); Writing – original draft (equal); Writing – review & editing (equal). **R. Varga**: Conceptualization (equal); Project administration (equal); Resources (equal); Software (equal); Supervision (equal); Validation (equal); Visualization (equal); Writing – review & editing (equal).

DATA AVAILABILITY

The data that support the findings of this study are available within the article.

REFERENCES

[1] A. Planes, L. Mañosa, and M. Acet, "Magnetocaloric effect and its relation to shape-memory properties in ferromagnetic Heusler alloys," J. Phys. Cond. Matter **21**, 233201 (2009).
[2] T. Krenke, M. Acet, E. F. Wassermann, X. Moya, L. Mañosa, and A. Planes, "Martensitic transitions and the nature of ferromagnetism in the austenitic and martensitic states of Ni–Mn–Sn alloys," Phys. Rev. B **72**, 014412 (2005).
[3] V. Sánchez-Alarcos, J. I. Pérez-Landazábal, V. Recarte, I. Lucia, J. Vélez, and J. A. Rodríguez-Velamazán, "Effect of high-temperature quenching on the magnetostructural transformations and the long-range atomic order of Ni–Mn–Sn and Ni–Mn–Sb metamagnetic shape memory alloys," Acta Materialia **61**, 4676 (2013).
[4] V. Vega, L. González, J. García, W. O. Rosa, D. Serantes, V. M. Prida, G. Badini, R. Varga, J. J. Suñol, and B. Hernando, "$Ni_{59.0}Mn_{23.5}In_{17.5}$ Heusler alloy as the core of glass-coated microwires: Magnetic properties and magnetocaloric effect," J. Appl. Phys. **112**, 033905 (2012).
[5] X. Zhang, M. Qian, Z. Zhang, L. Wei, L. Geng, and J. Sun "Magnetostructural coupling and magnetocaloric effect in Ni–Mn–Ga–Cu microwires," Appl. Phys. Lett. **108**, 052401 (2016).
[6] H. Zhang, M. Qian, X. Zhang, S. Jiang, L. Wei, D. Xing, J. Sun, L. Geng, "Magnetocaloric effect of Ni–Fe–Mn–Sn microwires prepared by melt-extraction technique," Materials & Design **114**, 1 (2017).
[7] P. J. Ibarra-Gaytán, L. Frolova, L. Galdun, T. Ryba, P. Diko, V. Kavecansky, J. L. Sánchez Llamazares, Z. Vargova, and R. Varga, "Glass-coated Ni_2MnGa microwires with narrow structural transition range and enhanced magnetocaloric effect at low fields," J. Alloys Compd. **786**, 65 (2019).
[8] A. Zhukov, M. Ipatov, J. Maria Blanco, P. Corté-Leon, and V. Zhukova, "Heusler-type glass-coated microwires: Fabrication, characterization, and properties," in *Magnetic Nano- and Microwires*, Woodhead Publishing Series in Electronic and

Optical Materials, 2nd ed., edited by M. Vázquez (Woodhead Publishing, 2020), Chap. 9, p. 255–294, ISBN: 9780081028322.
[9]Z. Chen, D. Cong, S. Li, Y. Zhang, S. Li, Y. Cao, S. Li, C. Song, Y. Ren, and Y. Wang, "External-field-induced phase transformation and associated properties in a $Ni_{50}Mn_{34}Fe_3In_{13}$ metamagnetic shape memory wire," Metals **11**, 309 (2021).
[10]M. Nazmunnahar, T. Ryba, J. J. del Val, M. Ipatov, J. González, V. Hašková, P. Szabó, P. Samuely, J. Kravcak, Z. Vargova, and R. Varga, "Half-metallic Ni_2MnSn Heusler alloy prepared by rapid quenching," J. Magn. Magn. Mater. **386**, 98 (2015).
[11]S. A. Baranov, V. S. Larin, and A. V. Torcunov, "Technology, preparation and properties of the cast glass-coated magnetic microwires," Crystals **7**, 136 (2017).
[12]P. Gorria, J. L. Sánchez Llamazares, P. Álvarez, M. J. Pérez, J. Sánchez Marcos, and J. A. Blanco, "Relative cooling power enhancement in magneto-caloric nanostructured Pr_2Fe_{17}," J. Phys. D: Appl. Phys. **41**, 192003 (2008).
[13]D. Wu, S. Xue, J. Frenzel, G. Eggeler, Q. Zhai, and H. Zheng, "Atomic ordering effect in $Ni_{50}Mn_{37}Sn_{13}$ magnetocaloric ribbons," Mater. Sci. Eng. A **534**, 568 (2012).
[14]H. Zhang, X. Zhang, M. Qian, L. Yin, L. Wei, D. Xing, J. Sun, and L. Geng, "Magnetocaloric effect in Ni–Fe–Mn–Sn microwires with nano-sized gamma precipitates," Appl. Phys. Lett. **116**, 063904 (2020).
[15]V. Franco, A. Conde, J. M. Romero-Enrique, and J. S. Blázquez, "A universal curve for the magnetocaloric effect: An analysis based on scaling relations," J. Phys. Cond. Matter **20**, 285207 (2008).